RSC Advances

ROYAL SOCIETY OF CHEMISTRY

www.rsc.org/advances

Novel green method of preparation of poly (ethylene oxide)/graphene nanocomposite using organic salt assisted dispersion

Siddheshwar B. Jagtap [a], Ramakant K. Kushwaha and Debdatta Ratna*

Polymer Science and Technology Centre, Naval Materials Research Laboratory, Shil-Badlapur Road, Anand nagar PO, Ambernath-421506, District -Thane, Maharashtra, India.

[a] Present address:- Polymer Science and Engineering Division, National Chemical Laboratory, Dr. Homi Bhabha Road, Pune- 411008, Maharashtra, India.

** Corresponding author email: ratnad29@hotmail.com, Tel: +91-251-2623036, Fax: +91-251-2623004*

Abstract

Nanocomposites of poly (ethylene oxide) (PEO) and graphene were made in aqueous solution using an organic salt containing a carboxylate ion and a carboxylic acid group. The cation corresponding to the carboxylate ion interacts with the π electron clouds of graphene through cation-π interaction and promotes the exfoliation of graphene sheets. The carboxylic acid group of the modifier forms H-bonding with the PEO and thereby improves interfacial adhesion. The effect of number of carbon atoms present in the modifier on its dispersing ability was investigated. It was observed that there exists an optimum number of carbon atoms present in the modifier with respect to the level of dispersion of graphene in the related nanocomposites as examined by scanning electron microscope (SEM) and transmission electron microscope (TEM). The mechanical properties of the nanocomposites having various concentration of graphene were evaluated and compared with the theoretical values using Halpin–Tsai model. The crystallization behavior of the PEO upon incorporation of modified graphene was studied by temperature modulated differential scanning colorimetry (MDSC) and discussed as well. The dispersion process used here is green as it does not require any toxic solvent or hazardous material for modification of graphene.

1. Introduction

Poly (ethylene oxide) has gained much importance among scientific communities due to its extensive applications in the areas like phase change materials[1,2], solid polymer electrolytes [3,4] (for battery, super capacitors and fuel cell) and crystallizable switching component for shape memory polymers (SMP).[5-7] In the recent years, attempts have been made to enhance the

performance of PEO for the applications (mentioned above) using various nanofillers.[8-11] The mechanical properties and ionic conductivity of PEO based solid electrolyte have been reported to be significantly improved due to incorporation of organoclay into the PEO matrix.[12–14] However, organoclay is one of the nanofiller which effectively improves the mechanical properties and provide materials with interesting array of properties. Although organoclay can significantly reinforce the PEO and improve ionic conductivity, it cannot improve thermal and electrical conductivity of the PEO. In addition to the reinforcing effect, the improvements in thermal and electrical conductivity are essential for the use of PEO as a phase change material and crystallizable switching component for SMP.

We have selected graphene as a nanofiller for modification of PEO because of its outstanding properties such as high surface area (2630~2965 m^2g^{-1}), high thermal conductivity (~3000$Wm^{-1}K^{-1}$), excellent electronic transport properties (~10^6 Scm^{-1}) and superior mechanical properties (~100 GPa).[15-20] Though, the graphene shows comparable mechanical properties to carbon nanotubes, still graphene is a better candidate in certain aspects, such as thermal and electrical conductivity.[21-23] However, effective reinforcement of graphene in the polymer matrix is hindered due to the strong tendency of aggregation of the graphene sheets.

A strategy commonly used to improve the dispersion of carbon based nanofiller is acid treatment.[24-27] This method is suffers from two problems: (a) it destroys π electron clouds to a certain extent which reduces the inherent conductivity and (b) use of concentrated acid increases handling risk and health hazard. In another strategy, carbon based nanofiller is modified by suitable functional molecules which involves physical adsorption on nanofiller surface (non-covalent functionalization).[20] The resulting interaction is primarily involves hydrophobic, Van der Waals, electrostatic forces and cation-π or π-π interactions. The cation-π or π-π interactions are found to be the best way to achieve good dispersion and interfacial interaction.[28-32] Majority of reports have been focused on nanofillers with various polymer matrices aiming a good dispersion and interfacial interaction.[27, 33-36]

In this paper, we have made an attempt to improve mechanical and thermomechanical properties of the PEO matrix using graphene by solution mixing technique. Non-covalent functionalization approach by using ionic modifier was used to achieve a uniform dispersion of graphene. Four dicarboxylic acid salts with different number of carbon atoms were used as the ionic modifiers. The present approach does not disturb the π electron clouds of graphene. Both

the modifier and the PEO matrix are soluble in water. Thus, this approach is environment friendly with no health hazards and can be adapted to any other water soluble polymers. The cation of the modifier can interact with π electron clouds of graphene via cation-π interaction and carboxyl group of the modifier can form H-bonding interaction with the PEO matrix. To our knowledge, till date no report is available in the literature on the use of cation-π interaction approach for dispersion of graphene in the PEO matrix and evaluation of its performance. The effect of number of carbon atoms of the modifiers on dispersion of graphene was investigated. Using the modifier with optimum number of carbon atoms, the effect of addition of graphene on the morphology, crystallization behavior, mechanical, and thermomechanical properties of the related PEO nanocomposites are discussed critically in this paper.

2. Experimental section

2.1. Materials

PEO with weight-average molecular weight of 600,000 g/mole was purchased from Sigma Aldrich Ltd, USA. Distilled water was used as a solvent. An adipic acid, succinic acid, suberic acid, sebacic acid and sodium hydroxide were purchased from Merck India Ltd and used as received. Graphene was procured from Reinste Nano Ventures India Ltd. The graphene was produced by the thermal exfoliation method having purity 99.5%, specific surface area 120-150 m^2/g and average particle size 6-8 nm.

2.2. Preparation of PEO/graphene nanocomposites

Initially, the dicarboxylic acids namely succinic acid, adipic acid, suberic acid and sebacic acid were converted to monocarboxylate acid salt by mixing 1:1 mole ratio of sodium hydroxide to dicarboxylic acids and are named as MC-1, MC-2, MC-3 and MC-4, respectively. Modified graphene was obtained by mixing the monocarboxylate acid salt and graphene in 1:1 ratio (w/w). PEO/graphene nanocomposites were prepared using various concentration of modified graphene by solution mixing method. A typical procedure of preparation of the PEO nanocomposite with 0.5wt% of MC-4 modified graphene is depicted as follows; 10 g of the PEO was dissolved in 100 mL distilled water in a 250 mL glass beaker and kept for 3 days without disturbing. Then, 0.5 wt % of MC-4 modified graphene was added into it. The mixture was then sonicated for 15 min by using a probe sonicator, keeping the beaker immersed in an ice bath. The,

PEO/graphene/MC-4 mixture was then poured into a suitable mold and kept in an air ventilated oven at 65 ^{o}C for 3 days for drying. A nanocomposite prepared is named as PEO/graphene (0.5wt %) /MC-4. Fig. 1 shows schematic representation of preparation PEO/graphene nanocomposites by solution mixing method.

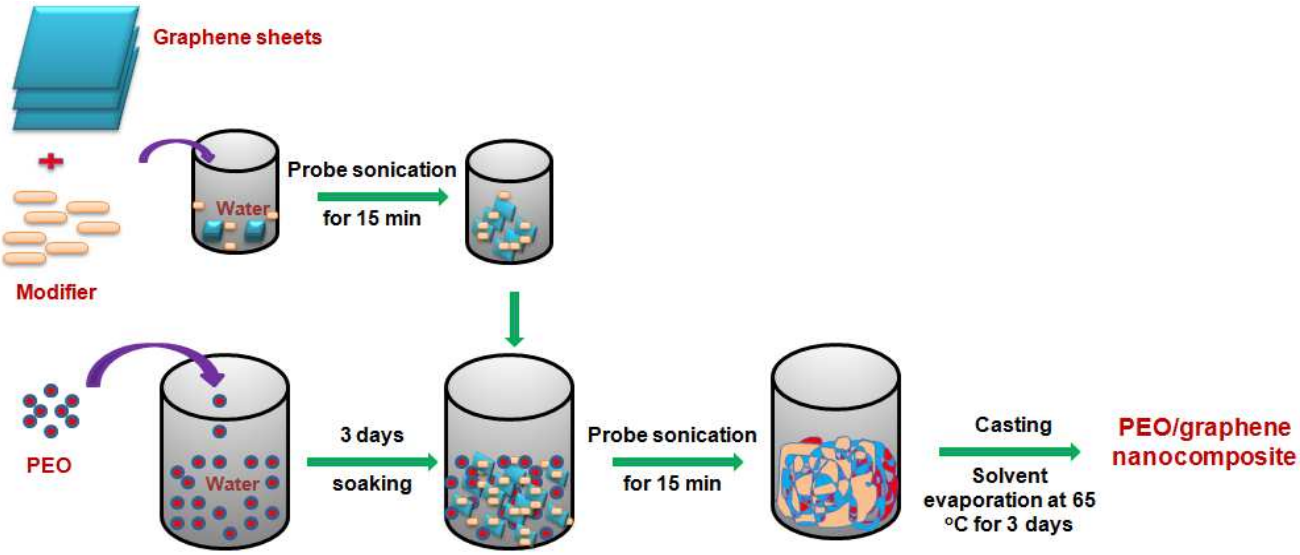

Fig. 1. Schematic representation of preparation of the PEO/graphene nanocomposite in water.

Similarly, PEO/graphene nanocomposites with 0.5wt % of unmodified graphene, MC-1 and MC-3 modified graphene were prepared by same procedure and designated as PEO/graphene (0.5wt %), PEO/ graphene (0.5wt %) /MC-1 and PEO/graphene (0.5wt %) /MC-3, respectively. Further, a series of PEO/graphene nanocomposites with increasing concentration (0.25 wt% - 1.25 wt %) of MC-2 modified graphene were also prepared to study the effect of concentration of graphene on the thermomechanical properties of the related nanocomposites.

2.3. Characterization

High resolution transmission electron microscope analysis of the PEO/graphene nanocomposites sample was conducted using a JEOL, (JEM-2100, Japan) electron microscope at 200 KV. Ultra-thin sections of the nanocomposite samples were prepared having thickness of 130-150 nm for TEM imaging by Leica ultracut microtome (Leica Mikrosysteme, GmbH, A-1170, Austria) using liquid nitrogen.

Field emission gun-scanning electron microscope (FEG-SEM, Zeissa Supra 40 VP, Germany) was used to study the fractured surface morphology of PEO/graphene nanocomposite samples.

The nanocomposite samples were quenched in the liquid nitrogen and cryogenically fractured to obtain the cross sections, which were sputter coated with carbon to avoid the charging before the SEM observation.

The tensile properties of the pure PEO and PEO/graphene nanocomposite samples were measured according to ASTM D-638 by a Universal Testing Machine (UTM, Hounsfield 50 KS Instron, UK). The crosshead speed was 100 mm per min and the gauge length was 50 mm. All the tests were performed at 27 ± 2 ^{o}C and the results are expressed in MPa. Four specimens of each sample were tested and the average of the obtained values was reported.

Fourier transform infrared (FTIR) spectra of graphene, MC-2 modified graphene, pure PEO and PEO/graphene (0.5wt%)/MC-2 nanocomposite samples was recorded using an attenuated total reflection (ATR) mode by using a Nicolet 510 FTIR spectrometer (Germany) over a scanning range from 800 to 3600 cm^{-1} with a nominal resolution of 2 cm^{-1} to discuss the interaction between the modifier, graphene and PEO. For each spectrum 64 runs were collected and averaged.

Crystallization behavior of pure PEO and PEO/graphene nanocomposite samples was studied using MDSC (TA instruments Q100 series, USA). About 6-10 mg of sample was placed in an aluminum pan and heated from room temperature to 100 ^{o}C and cooled to 0 ^{o}C with a heating/cooling rate 5 ^{o}C per min. The reference was an empty aluminum pan. Melting point (T_m), crystallization temperature (T_c), enthalpy of crystallization (ΔH_c) and percentage of crystallinity (X_c) were calculated from the DSC plots.

Dynamic mechanical analysis (DMA) of the pure PEO and PEO/graphene nanocomposite samples was carried out using a dynamic mechanical thermal analyzer (DMTA, MK IV, Rheometric Scientific, USA). The test specimen was cooled to - 100 ^{o}C, allowed to stabilize and then heated at a rate of 3 °C per min to 30 ^{o}C. Liquid nitrogen was used for sub-ambient temperatures. Storage modulus, loss modulus and tan δ were obtained by using a dual cantilever mode for the sample of size 30 x 10 x 2 mm^3 using a fixed frequency of 1 Hz.

Thermogravimetric analysis (TGA) of the graphene, MC-2 modified graphene, pure PEO and PEO/graphene (0.5wt%) /MC-2 nanocomposite samples was carried out using a thermogravimetric analyzer, TA Instrument (TGA Q500, USA). 6 - 8 mg of sample was heated from room temperature to 800 ^{o}C at a heating rate of 20 ^{o}C per min under nitrogen atmosphere.

3. Results and Discussion

Fig. 2 shows TEM photographs for PEO/graphene (0.5 wt %), PEO/graphene (0.5 wt %) /MC-1, PEO/graphene (0.5 wt %) /MC-2, PEO/graphene (0.5 wt %) /MC-3 and PEO/graphene (0.5 wt %) /MC-4 nanocomposites. In a nanocomposite made without modifier [PEO/graphene (0.5 wt %)], we can see that the graphene sheets are highly aggregated (Fig. 2a). This indicates the absence of interaction between the unmodified graphene and the PEO. When the modifier was mixed with graphene, a significant improvement in dispersion level of graphene was obtained (Fig. 2b-e). This can be attributed to the presence of cation-π interaction and H-bonding interaction. The cation (Na^+) of modifier interacts with the π electron clouds of graphene via cation- π interaction and –OH group of the modifier forms H–bonding interaction with the PEO. This type of interaction reduces the strong Van der Waal interactions within the graphene sheets and promotes their exfoliation.

Among the four nanocomposites, the extent of exfoliation of graphene sheets is found to be the highest in PEO/graphene (0.5wt %) /MC-2 nanocomposite. TEM analysis indicates that the graphene sheets are exfoliated into a single layer throughout the image (Fig. 2c). PEO/graphene (0.5wt %) /MC-3 nanocomposite also shows similar morphology with a lesser extent of exfoliated graphene sheets (Fig. 2d). The approximate thickness of a single graphene sheet was estimated using ImageJ software and found to be 1.4 nm. PEO/graphene (0.5 wt %) /MC-1 and PEO/graphene (0.5wt %) /MC-4 nanocomposites did not show exfoliated graphene. This indicates that the number of carbon atom of the modifier played an important role on the resulting morphology as a result of dispersion. The modifier with six carbon atoms is found to be the optimum in achieving exfoliation of graphene sheets into the PEO matrix.

The improvement of level of dispersion of graphene due to the addition of an ionic modifier (with a carboxyl and carboxylate group) can be explained by considering two factors namely polarity matching and the formation of salts with one carboxylate ions.[34, 35] For polarity matching with the PEO, modifier with higher numbers of carbon atoms are required. Here, the modifiers are monocarboxylic acid salts having different number of carbon atoms. For the formation of one carboxylate ions, a dicarboxylic acid was modified with a half equivalent of sodium hydroxide. So, there is always a possibility of the formation of dicarboxylate ions. For achieving both exfoliation and interfacial adhesion, the formation of a salt with one carboxylate and one carboxylic group is most desirable. However, with increase in number of carbon atoms

of the modifier, the probability of the formation of a salt with one carboxylate ion decreases. The formation of dicarboxylate ions is more for the modifier with higher number of carbon atoms (i.e. MC-4). The modifier (MC-2) having carbon atom six showed suitability in terms of polarity matching with the PEO and the formation of one carboxylate ion. That is why an excellent dispersion of graphene sheets was seen from TEM image (Fig. 2c) of the PEO/graphene (0.5wt %) /MC-2 nanocomposite. Fig. 3 shows schematic representation of the cation-π interaction between MC-2 and graphene, H-bonding interaction of –COOH groups of MC-2 with the PEO. Abovementioned morphological features clearly explained the role of number of carbon atoms of the modifier on exfoliation of graphene sheets into the PEO which was further supported by tensile properties discussed, subsequently.

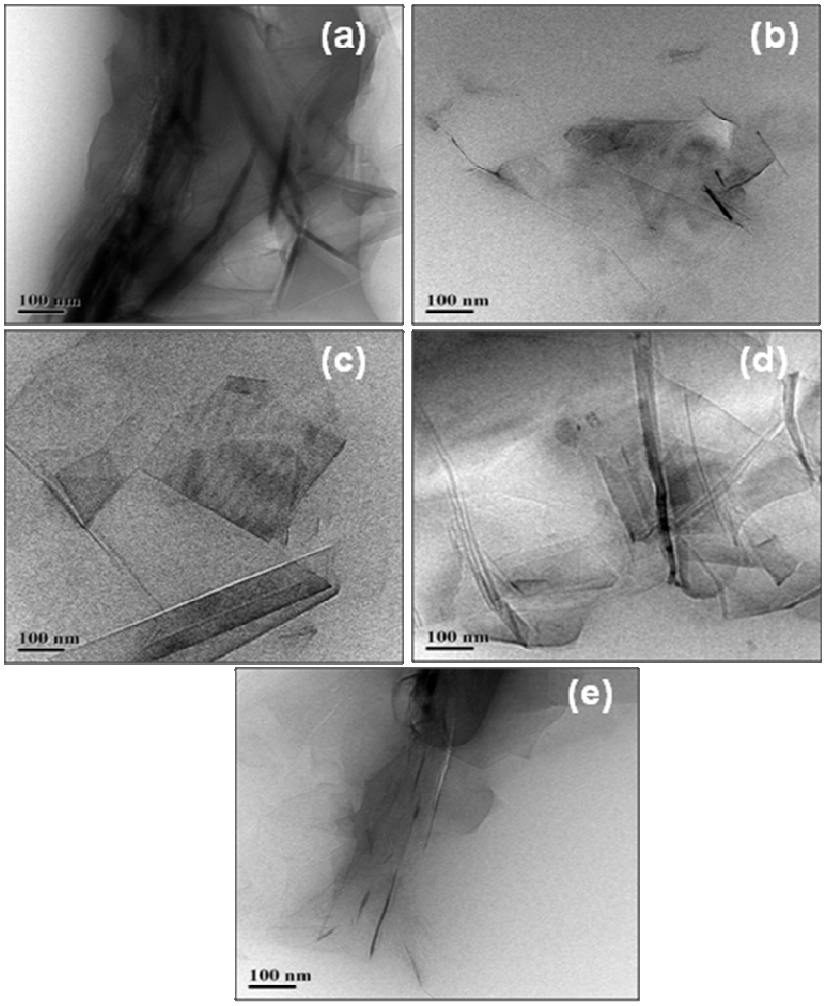

Fig. 2. TEM photographs of (a) PEO/graphene (0.5 wt %), (b) PEO/graphene (0.5 wt %) /MC-1, (c) PEO/graphene (0.5 wt %) /MC-2, (d) PEO/graphene (0.5 wt %) /MC-3 and (e) PEO/graphene (0.5 wt %) /MC-4 nanocomposites.

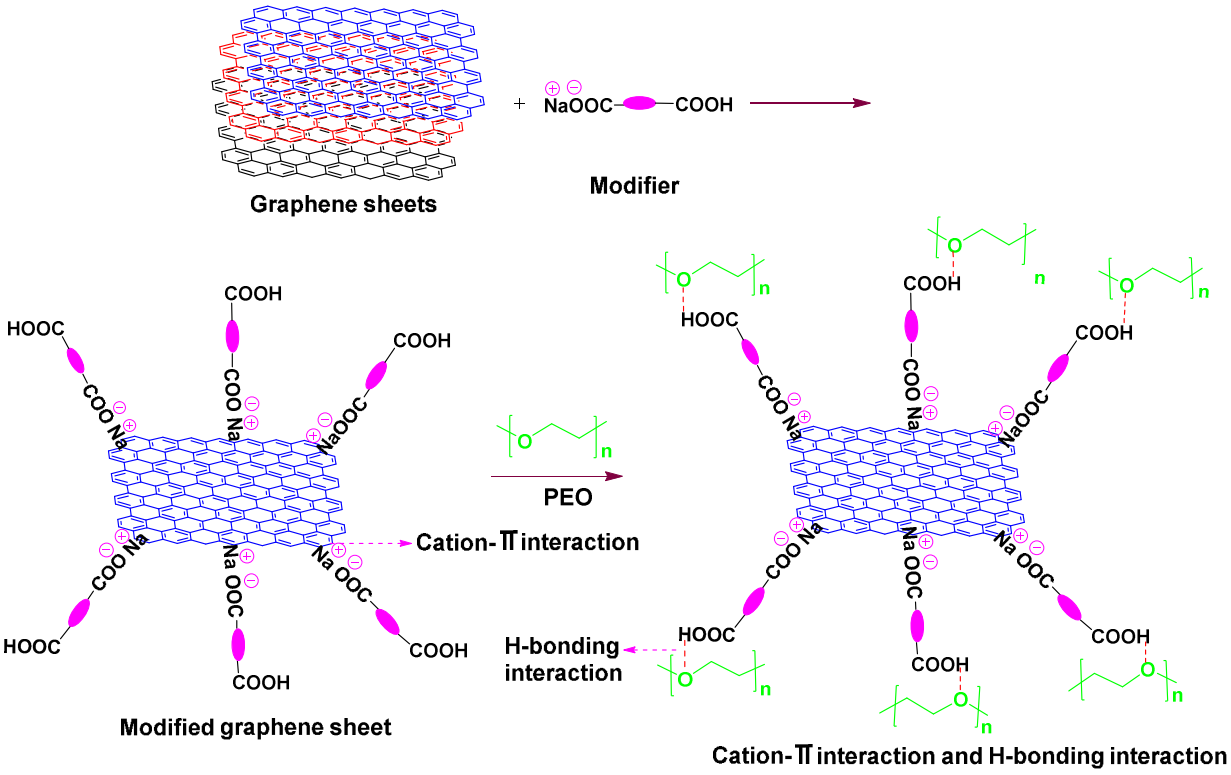

Fig.3. Schematic representation of the cation-π interaction between modifier and graphene and H-bonding interaction of –COOH groups of modifier with the PEO.

As discussed above, good dispersion of graphene is a result of cation-π interaction between the modifier and graphene and H-bonding interaction between the modifier and PEO. We have used FTIR analysis to study the existence of cation-π interaction and H-bonding interaction. Fig. 4 shows the FTIR spectra of MC-2, MC-2 modified graphene, pure PEO and PEO/graphene (0.5wt %) /MC-2 nanocomposite. The peaks at 1710 cm^{-1} and 1563 cm^{-1} correspond to the stretching of C=O group of carboxylic acid and carboxylate ion of the MC-2. The C=O group of carboxylate ion exhibits a peak at 1563 cm^{-1}, which is lower than the characteristic peak for carboxylic acid group at 1710 cm^{-1}. This is because the negative (–ve) charge on oxygen atom of carboxylate ion undergoes dislocation and reduces the bond strength of C=O group and results a reduction in the wave number. After the modification of graphene with MC-2, the carboxylate ion peak is shifted toward a higher wave number, i.e. from 1563 cm^{-1} to 1580 cm^{-1} (Fig.4b). This shift of carboxylate ion peak is attributed to the strong electrostatic interaction between the cation (Na^{+}) with the π electron clouds of graphene (known as cation - π interaction). This interaction reduces the effectiveness of dislocation of negative charge on oxygen atom resulting

in an increase in wavenumber of carboxylate ion (C=O) peak. The shift in characteristic C=O group (carboxylic acid) stretching peak from 1710 cm^{-1} to 1740 cm^{-1} suggests H-bonding interaction between MC-2 with the PEO (Fig 4d). Note that pure PEO does not show any peak at 1740 cm^{-1}.

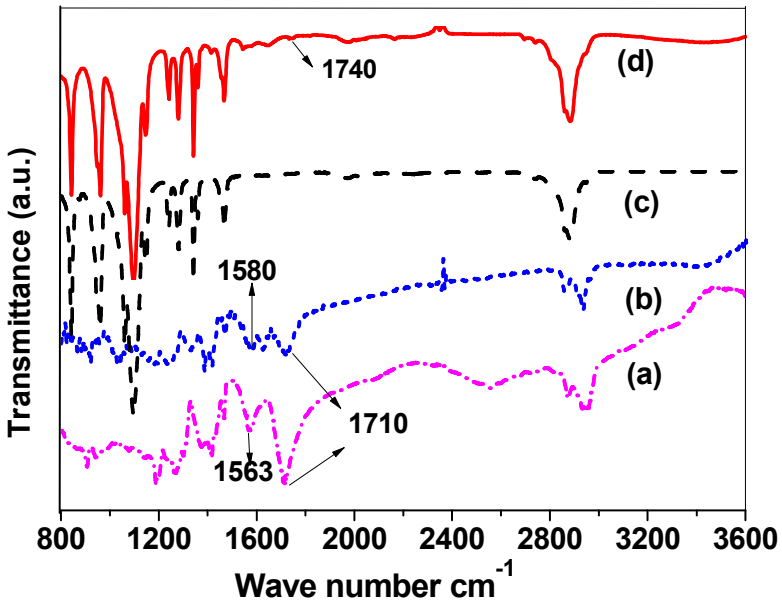

Fig.4. FTIR spectra of (a) the modifier MC-2, (b) MC-2 modified graphene, (c) pure PEO and (d) PEO/graphene (0.5wt %) /MC-2 nanocomposite.

Unlike other thermoplastics polymers, mechanical properties of the PEO-based nanocomposites are not reported much, because they are not used for high strength applications. Reinforcement of the PEO is needed to improve its mechanical properties for the development of high performance of PEO-based nanocomposites. Graphene can be a potential candidate for improving the mechanical properties of PEO based electrolytes and SMP systems. Therefore, in this work, we studied the mechanical properties of the PEO/graphene nanocomposites and discussed. The tensile properties of the pure PEO and the related nanocomposite samples are tabulated in Table 1. We can see that the PEO /graphene (0.5 wt %) nanocomposite does not show much improvement in the tensile properties because of the poor dispersion of unmodified graphene (as evident from TEM, Fig. 2a discussed above). On the other hand, all the PEO nanocomposites containing modified graphene exhibit a significant improvement in the tensile

properties. Interestingly, the improvement is achieved in all respects (tensile strength, tensile modulus and elongation at break).

Table 1. Tensile properties of the pure PEO and PEO/graphene nanocomposites.

Samples	Tensile strength (MPa)	Tensile modulus (MPa)	Elongation at break (%)
PEO	**11.0 ± 0.5**	**117 ± 2**	**376 ± 20**
PEO/Graphene (0.5wt %)	**11.6 ± 0.7**	**208 ± 4**	**590 ± 25**
PEO/ Graphene (0.5wt%)/MC-1	**14.7 ± 0.4**	**322 ± 6**	**694 ± 15**
PEO/ Graphene (0.5wt%)/MC-2	**16.4 ± 0.6**	**373 ± 8**	**690 ± 23**
PEO/ Graphene (0.5wt%)/MC-3	**12.9 ± 0.3**	**281 ± 4**	**752 ± 16**
PEO/ Graphene (0.5wt%)/MC-4	**11.7 ± 0.2**	**273 ± 5**	**717 ± 10**

Among the nanocomposites prepared, a PEO/graphene (0.5 wt %) /MC-2 nanocomposite offers the best performance. It showed around 50 %, 220% and 83% increase in the tensile strength, tensile modulus and elongation at break, respectively. This increase in the tensile properties is a result of good dispersion of graphene in the PEO (as confirmed by TEM discussed above). Due to high aspect ratio, high surface area and platelets like structure, a graphene can establish a strong interfacial interaction with the modifier and the PEO matrix. Both the good dispersion and strong interfacial interaction arise from the cation-π interaction and H-bonding interaction between the modifier, graphene and the PEO as shown in Fig. 3.

We made a series of PEO/graphene nanocomposites with increasing concentrations of MC-2 modified graphene to study the effect of modifier MC-2 on tensile properties of the nanocomposites. The representative stress-strain profiles of the pure PEO, PEO/graphene (0.5wt %), PEO/graphene (0.5wt %) /MC-2 and PEO/graphene (0.75wt %) /MC-2 nanocomposites are shown in Fig. 5. The results are summarized in Table 2. It can be seen that the tensile properties of PEO nanocomposites increases with increasing concentration of MC-2 modified graphene up to 0.75 wt% and thereafter decreases. The PEO/graphene (0.75wt %) /MC-2 nanocomposite shows higher % elongation at break as compared to the pure PEO and all other nanocomposites. It shows around 67%, 301% and 103% increase in the tensile strength, tensile modulus and elongation at break, respectively. The improvement in the tensile properties can be attributed to the uniform dispersion of graphene and strong interfacial interaction with the PEO. This

interaction effectively transfers the load from the PEO to the graphene sheet, thereby enhanced tensile properties. The decrease in tensile properties beyond 0.75 wt% of MC-2 modified graphene can be attributed to the increase in agglomeration of graphene (as discussed subsequently by SEM and TEM).

Table 2. Tensile properties of PEO/graphene nanocomposites with different concentration of MC-2 modified graphene.

MC-2 modified graphene (wt %)	Tensile strength (MPa)	Tensile modulus (MPa)	Elongation at break (%)
0	11.0 ± 0.5	117 ± 2	376 ± 20
0.25	15.8 ± 0.2	306 ± 5	552 ± 18
0.5	16.4 ± 0.6	373 ± 8	690 ± 23
0.75	18.1 ± 0.4	470 ± 6	760 ± 20
1	15.4 ± 0.3	387 ± 4	766 ± 22
1.25	14. 1 ± 0.2	314 ± 3	660 ± 15

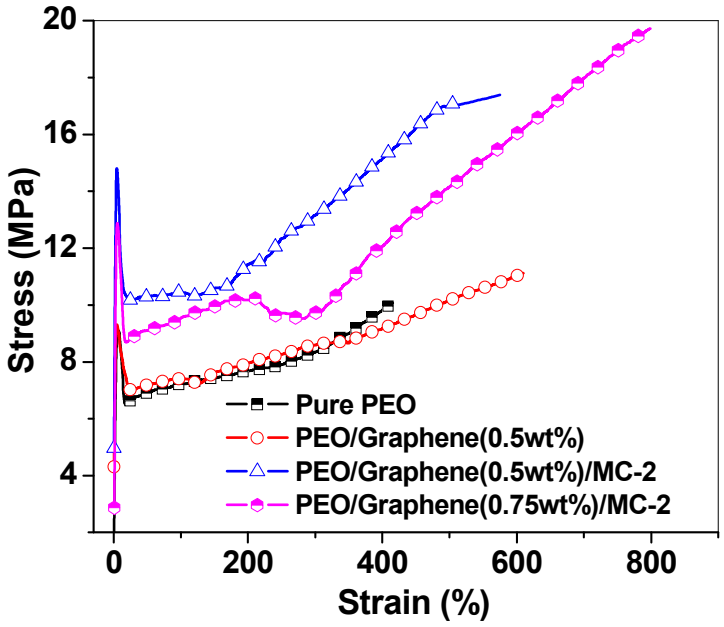

Fig.5. Stress vs. strain profile of the pure PEO, PEO/graphene (0.5wt %), PEO/graphene (0.5wt %) /MC-2 and PEO/graphene (0.75wt %) /MC-2 nanocomposites.

We have analyzed PEO/graphene nanocomposite samples by the SEM and TEM to study the effect of higher concentration of MC-2 modified graphene on dispersion level. SEM photographs

of cryogenically fractured surface of the PEO/ graphene (0.5wt %), PEO/ graphene (0.5wt %) /MC-2, PEO/ graphene (0.75 wt %) /MC-2 and PEO/ graphene (1.25 wt %) /MC-2 nanocomposites are displayed in Fig. 6. From SEM photographs of PEO/graphene (0.5wt %) and PEO/ graphene (1.25 wt %) /MC-2 nanocomposites, we can see that the fracture did not occur preferentially at the PEO-graphene interface (Fig. 6a and 6d). Whereas, PEO/ graphene (0.5wt %) /MC-2 and PEO/ graphene (0.75wt %) /MC-2 nanocomposites (Fig. 6b and 6c) exhibit fully embedded graphene in the PEO matrix. This observation confirmed that the six carbon atoms of MC-2 not only plays an important role in improving the dispersion but also helps to establish a strong interfacial interaction with the PEO.

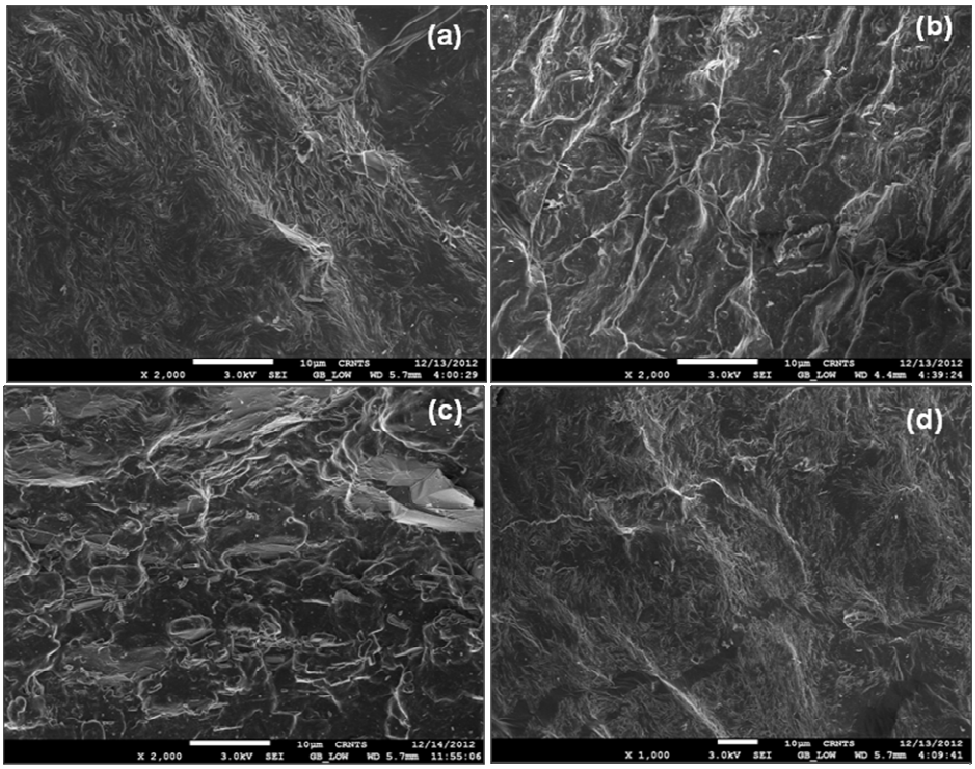

Fig.6. SEM photographs of cryogenically fractured surface of (a) PEO/ graphene (0.5wt %), (b) PEO/ graphene (0.5wt %) /MC-2, (c) PEO/ graphene (0.75 wt %) /MC-2 and (d) PEO/ graphene (1.25 wt %) /MC-2 nanocomposites.

In TEM images, PEO/ graphene (0.75wt %) /MC-2 nanocomposite exhibits the exfoliation of graphene into a single sheet (Fig. 7a). On the other hand, the morphology obtained for the PEO/ graphene (1.25 wt %) /MC-2 (Fig. 7b) nanocomposite clearly indicates that at a higher

concentration of graphene, it is difficult to prevent the agglomeration. This explains why the tensile properties of PEO nanocomposites drop down when concentration of graphene goes beyond 0.75 wt%.

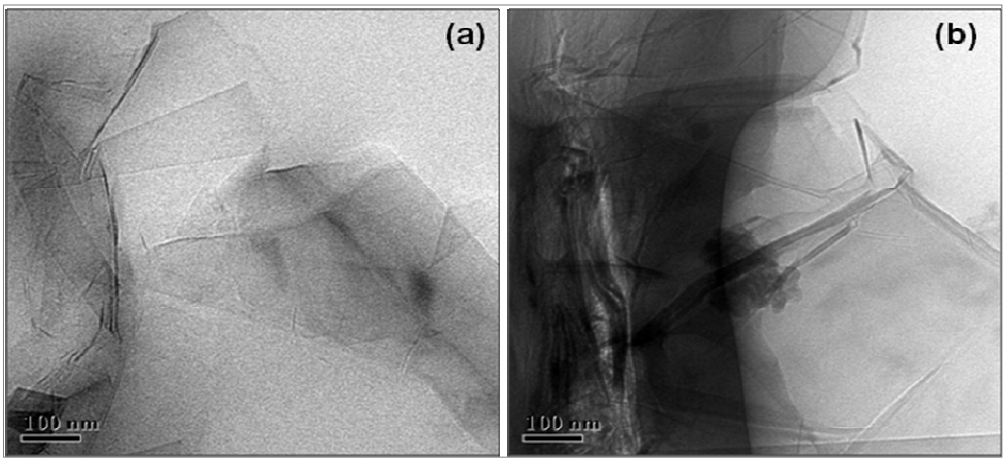

Fig.7. TEM images of (a) PEO/ graphene (0.75wt %) /MC-2 and (b) PEO/ graphene (1.25 wt %) /MC-2 nanocomposites.

Further, Halpin-Tsai model was used to find out the modulus of the PEO/graphene nanocomposites. This model is widely used for predicting the modulus of unidirectional ($E_{||}$) or randomly distributed (E_r) filler-reinforced nanocomposites.[37-40] The equations for unidirectional or randomly oriented graphene sheets in the polymer matrix are given as follows:

$$E_r = E_m\left[\frac{3}{8}\left(\frac{1+M_L f\phi_c}{1-M_T f\phi_c}\right)+\frac{5}{8}\left(\frac{1+2M_T\phi_c}{1-M_T\phi_c}\right)\right] \quad (1)$$

$$E_{ll} = E_m\left(\frac{1+M_L f\phi_c}{1-M_L f\phi_c}\right) \quad (2)$$

$$M_L = \left(\frac{\frac{E_g}{E_m}-1}{\frac{E_g}{E_m}+f}\right) \quad (3)$$

$$M_T = \left(\frac{\frac{E_g}{E_m}-1}{\frac{E_g}{E_m}+2}\right) \quad (4)$$

$$f = \left(\frac{2\,l_g}{3\,t_g}\right) \quad (5)$$

Where, the E_g and E_m are Young's modulus of the graphene and the PEO matrix, respectively. The l_g and t_g represent length and thickness of the graphene sheet, respectively and ϕ_c is the volume fraction of graphene in the nanocomposites. The Young's modulii (E) of the graphene sheet and PEO matrix are 0.25 TPa[41] and 117 MPa (as determined by tensile test), respectively. Densities of the PEO matrix and graphene sheets are 1.21 g cm^{-3} and 2.26 g cm^{-3}, respectively. The statistical average value of l_g and t_g are 0.276 μm and 1.4 nm respectively, as determined by TEM. All the parameters were substituted into equation (1)–(5) and Young's modulus can be calculated assuming two possible distribution of graphene: randomly distributed as 3D network throughout the polymer matrix, and aligned parallel (as 2D network) to the surface of sample.[37,38,42] Fig. 8 shows comparison of experimental and calculated Young's modulus for the PEO/graphene nanocomposites. It can be noted that the experimental Young's modulus agrees well with the theoretical value calculated assuming random distribution of graphene throughout the PEO matrix.

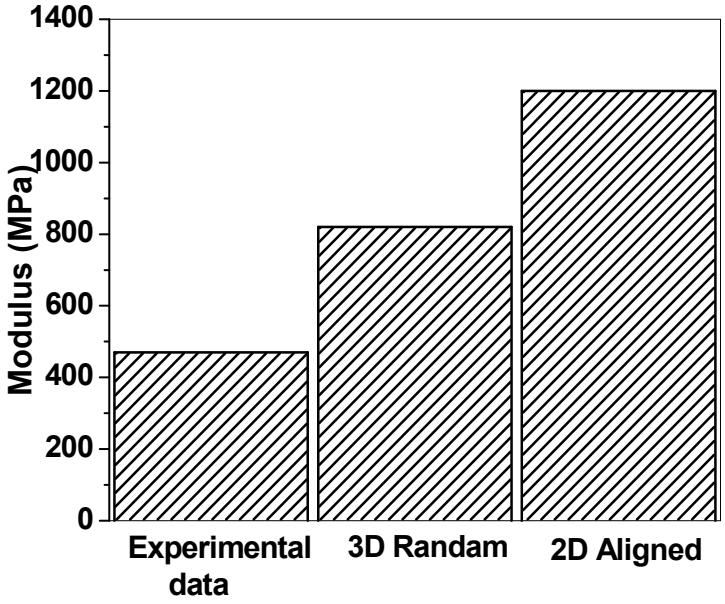

Fig.8. Comparison of the experimental modulus and calculated modulus (3D random and 2D aligned) for the PEO/graphene nanocomposites.

We studied the dynamic mechanical properties, crystallization behavior and thermal stability of PEO/ graphene nanocomposites in order to investigate the effect of modifier MC-2.

The storage moduli vs. temperature and loss moduli vs. temperature plots of the pure PEO, PEO/graphene (0.5wt %), PEO/ graphene (0.5wt %) /MC-2, PEO/graphene (0.75wt %) /MC-2, PEO/graphene (1wt %) /MC-2, and PEO/graphene (1.25 wt %) /MC-2 nanocomposites are shown in Fig. 9a and 9b, respectively. PEO/ graphene (0.5wt %) nanocomposite shows a moderate improvement in the storage modulus as compared to the pure PEO. On the other hand, storage modulus of the PEO/graphene/MC-2 nanocomposite is increased with increasing graphene concentration up to 0.75 wt% and decreased thereafter. This can be attributed to a strong interfacial interaction of graphene with the PEO and high aspect ratio of the graphene sheet which helps in transferring load across the PEO-graphene interface.

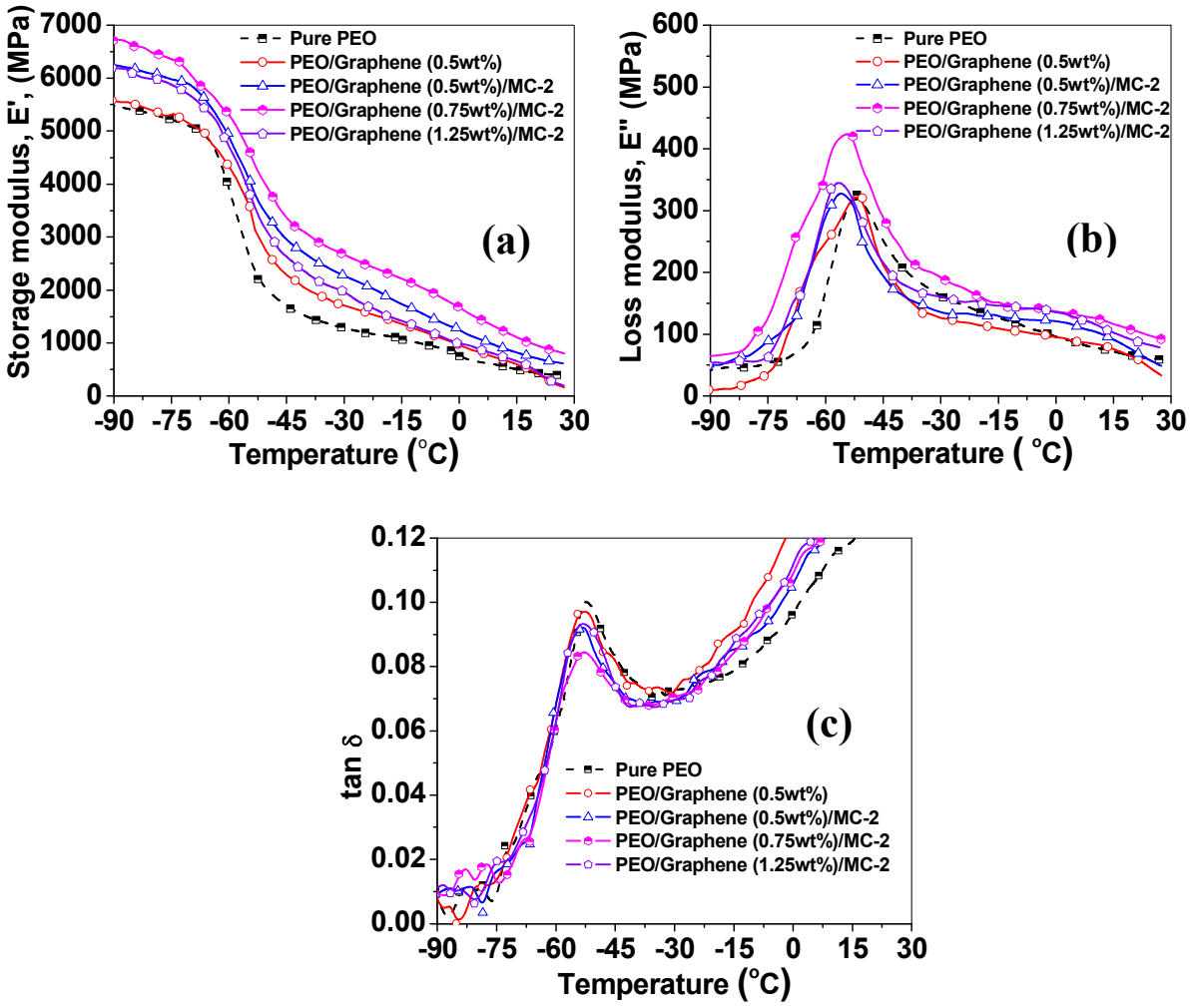

Fig.9. (a) Storage modulii vs. temperature, (b) Loss modulus vs. temperature and (c) tan δ vs. temperature plots of the pure PEO, PEO/graphene (0.5wt %), PEO/ graphene (0.5wt %) /MC-2, PEO/graphene (0.75wt %) /MC-2, PEO/graphene (1.25 wt %) /MC-2 nanocomposites.

Further, all the PEO/ graphene nanocomposites show higher loss modulus (peak height) as compared to the pure PEO (Fig 9b). This can be attributed to the shearing action between the graphene sheets and PEO chains leading to a higher loss modulus. This behavior is quite different from that observed for conventional fillers, which always reduces the loss modulus. The higher damping loss can be explained by considering the phenomenon similar to "constrained layer damping" (CLD) concept.[9, 29, 30, 43] The presence of graphene sheets also resulted in reduction of the tan δ peak height. This indicates the increase in stiffness and rigidity of the nanocomposites (Fig. 9c) which leads to the restricted segmental motions at the PEO-graphene interfaces.[44]

In Fig. 10, we compared DSC crystallization plots of the pure PEO and selected PEO nanocomposite samples prepared using varying concentrations (wt %) of MC-2 modified graphene. The heat of crystallization values of the composite samples (ΔH_c) were calculated from the formula given below:

$$\Delta H_c = \frac{(\Delta H_c)_{total}\, X\, 100}{w\, x\, y} \qquad (6)$$

where, $(\Delta H_c)_{total}$ is obtained from the peak area of DSC cooling curve, w is the weight of sample taken for DSC experiment and y is the concentration of PEO (wt%) in the nanocomposite. The percentage of crystallinity (X_c) of the nanocomposites can be calculated from the following formula:

$$X_c = \Delta H_C / \Delta H^o_c \qquad (7)$$

Where ΔH_c is the specific heat of crystallization of the nanocomposite and ΔH^o_c is the specific heat of crystallization of 100% crystalline PEO (205 Jg^{-1}).[45] Melting temperature (T_m), crystallization temperature (T_c), heat of crystallization $(\Delta H_c)_{total}$ and X_c of all the nanocomposite samples are tabulated in Table 3. It was observed that the nanocomposites containing MC-2 modified graphene exhibit higher T_c than that of the pure PEO. In the nanocomposites, graphene sheets are well dispersed as evidenced by TEM. Hence they do not exert any steric hindrance by blocking the crystal growth fronts during the crystallization process.[20] The T_c was reported to be decreased in case of PEO/phenolic blends [46] and nanocomposites made using organoclay [47] and unmodified MWCNT [48] due to the steric hindrance caused by the fillers. The higher T_c of the nanocomposites can be attributed to the nucleation effect of well dispersed graphene. This also

explains the higher crystallinity of the nanocomposites as compared to the pure PEO. It may be noted that the melting point decreases as a result of incorporation of graphene into PEO. This can be explained by considering the fact that the sizes of the PEO crystallites in the nanocomposite tend to decrease as a result of the nucleation effect of the modified graphene[20]. Because of the presence of higher number of smaller (compared the crystallite in pure PEO) crystallites, the nanocomposite shows higher crystallinity but lower melting temperature as compared to the pure PEO.

Table3. DSC parameters of the pure PEO and PEO/graphene/MC-2 nanocomposites containing varying concentration of the graphene.

MC-2 modified graphene (wt %)	T_c (^{o}C)	T_m (^{o}C)	ΔHc (J/g)	Percentage of crystallinity (X_c)
0	42.1	67.2	140	68
0.25	47.3	64.7	150	73
0.5	47.9	67.4	158	77
0.75	48.0	65.6	163	79
1	46.8	64.7	156	76
1.25	46.1	63.6	151	72

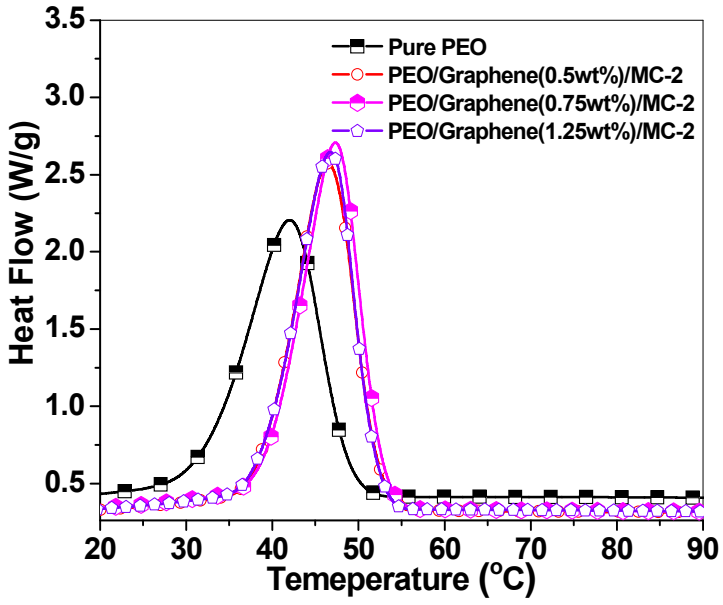

Fig.10. Heat flow vs. temperature plots of the pure PEO and selected PEO nanocomposite samples prepared with different wt% of MC-2 modified graphene.

Fig. 11 shows the thermal stability of unmodified graphene, MC-2 modified graphene, pure PEO and PEO/ graphene (0.75wt %) /MC-2 nanocomposite. As expected, graphene does not show any significant degradation up to 700 ^{o}C. On the other hand, the modified graphene starts initial degradation at 194 ^{o}C and maximum degradation (46 % weight loss) was obtained at 700 ^{o}C. This is due to the presence of organic modifier on the surface of graphene. Further, when we compared thermal stability of pure PEO and PEO nanocomposite containing 0.75wt% of MC-2 modified graphene. The pure PEO starts degrading at 240 ^{o}C and the maximum degradation was obtained at 400 ^{o}C. After addition of 0.75 wt% of graphene to the PEO, initial degradation and maximum degradation temperature were enhanced by 110 ^{o}C (350 ^{o}C) and by 30 ^{o}C (430 ^{o}C), respectively. This significant improvement in thermal stability of PEO/graphene (0.75wt %) /MC-2 nanocomposite as compared to the pure PEO could be attributed to the so called ‘‘tortuous path’’ due to the graphene, which delayed the escape of volatile degradation products and also char formation.[49, 50]

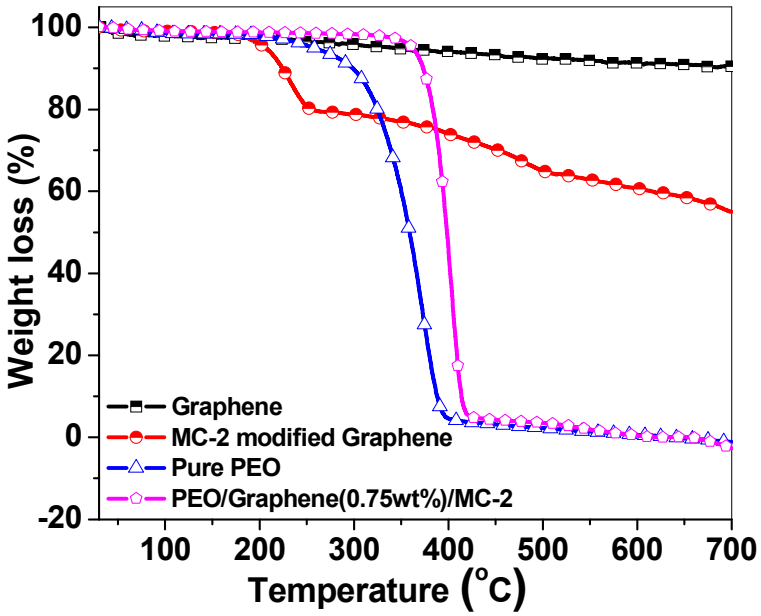

Fig.11. TGA thermograms of unmodified graphene, MC-2 modified graphene, pure PEO and PEO/ graphene (0.75wt %) /MC-2 nanocomposite.

4. Conclusions

A green method for synthesis of a nanocomposite of poly (ethylene oxide) (PEO) and graphene has been demonstrated. The optimum number of carbon atoms of the modifier used to enhance the dispersion of graphene in the PEO matrix was found to be six. The modifier is soluble in water and interacts with the graphene and PEO via cation-π interaction and H-bonding interaction. The graphene was found to be highly exfoliated and thickness of single layer was 1.4 nm. The incorporation of small amount of graphene (0.5-0.75 wt %) offers a significant reinforcement coupled with enhanced thermal stability. The well dispersed graphene sheets act as nucleation centres and increases the crystallinity of the nanocomposites.

References

1. C. Qi and P. Liu, *Eur. Polym. J.*, 2006, **42**, 2931.
2. K. Pielichowska and K. Pielichowski, *J. Appl. Polym. Sci*., 2010, **116**, 1725.
3. Applications of Electroactive Polymers; Scrosati, B., Ed.; *Chapman & Hall*: New York, 1993, p 251.
4. W, Wieczorek, D. Raduacha, A. Zalewska and J. K. Stevens, *J. Phys. Chem. B.,* 1998, **102**, 8725.
5. G. Liu, C. Guan, H. Xia, F. Guo, X. Ding and Y. Peng, *Macromol. Rapid. Commun.,* 2006, **27**, 1100.
6. D. Ratna and J. Karger-Kocsis, *J. Mater. Sci.,* 2008, **43**, 254.
7. T.N. Abraham, D. Ratna, S. Siengchin and J. Karger-Kocsis, *Polym. Eng. Sci.,* 2009, **49**, 379.
8. D. Ratna, S. Divekar, P. Sivaraman, A. B. Samui and B. C. Chakraborty, *Polym. Int.,* 2007, **56**, 900.
9. D. Ratna, T. N. Abraham, S. Siengchin and J. Karger-Kocsis, *J. Polym. Sci. Part B: Polym. Phys.,* 2009, **47**, 1156.
10. W. E. Mahmoud, *Eur. Polym. J.,* 2011, **47**, 1534.
11. S. B. Jagtap and D. Ratna, *eXPRESS Polym. Lett*., 2013, **4**, 329.
12. H. B. Zhang, W.G. Zheng, Q. Yan, Y. Yang, J. W. Wang and Z. H. Lu, *Polymer,* 2010, **51**, 1191.

13. F. Schedin, A. K. Geim, S. V. Morozov, E. W. Hill, P. Blake and M. I. Katsnelson, *Nat. Mater.,* 2007, **6,** 652.
14. L .L. Zhang, R. Zhou and X. S. Zhao. *J. Mater. Chem.,* 2010, **20**, 5983.
15. K. S. Novoselov, A. K. Geim, S. V. Morozov, D. Jiang, Y. Zhang and S. V. Dubonos, *Science,* 2004, **306,** 666.
16. K. S. Novoselov, A. K. Geim, S. V. Morozov, D. Jiang, M. I. Katsnelson and I. V. Grigorieva, *Nature,* 2005, **438,** 197.
17. J. J. Mack, L. M. Viculis, A. Ali, R. Luoh, G. Yang, H. T. Hahn, F. K. Ko and R. B. Kaner, *Adv. Mater*., 2005, **17**, 77.
18. K. S. Subrahmanyam, S. R. C. Vivekchand, A. Govindaraj and C.N.R. Rao, *J. Mater. Chem.,* 2008, **18**, 1517.
19. S. Stankovich, D. A. Dikin, G.H.B. Dommett, K.M. Kohlhaas, E. J. Zimney, E. A. Stach, R. D. Piner, S. T. Nguyen and R.S. Ruoff, *Nature,* 2006, **442**, 282.
20. H. B. Lee, A. V. Raghu, K..S. Yoon and H. M. Jeong, *J. Macromo. Sci. Part B: Physics,* 2010*,* **49**, 802.
21. N. Tombros, C. Jozsa, M. Popinciuc, H. T. Jonkman and B. J. van Wees, *Nature,* 2007, **448,** 571.
22. F. Ji, Y. L. Li, J. M. Feng, D. Su, Y. Y. Wen and Y. Feng, *J. Mater. Chem.,* 2009, **19,** 9063.
23. A. A. Balandin, S. Ghosh, W. Z. Bao, I. Calizo, D. Teweldebrhan and F. Miao, *Nano Lett.,* 2008, **8**, 902.
24. Y. Shin-Yi, M. M. Chen-Chi, T. Chih-Chun, H. Yen-Wei, L. Shu-Hang, H. Yuan-Li, T. Hsi-Wen, L. Tzong-Ming and C. Kuo-Chan, *Carbon*, 2010, **48**, 592.
25. Y. Zheng, A. Zhang, Q. Chen, J. Zhang and R. Ning, *Mater. Sci. and Eng. A,* 2006, **435**, 145.
26. M. Abdalla, D. Derrick, D. Adibempe, E. Nyairo, P. Robinson and G. Thompson, *Polymer,* 2007, **48**, 5662.
27. T. Kuila, S. Bose, A. K. Mishra, P. Khanra, N. H. Kim and J. H. Lee, *Prog. in Mater. Sci.,* 2012, **57**, 1061.
28. R. B. Naik, S.B. Jagtap, R.S. Naik, R.G. Malvankar and D. Ratna, *Prog. in Org. Coat.,* 2014, **77**, 1883.

29. D. Ratna, S. B. Jagtap, Ritu Rathor, R. K. Kushwaha, N. Shimpi and S. N. Mishra, *Polym. Compos*., 2013, **34**, 1003.
30. D. Ratna**,** S. B. Jagtap and T Abraham, *Polym. Eng. and Sci.,* 2013, **53**, 555.
31. E. Y. Choi, T. H. Han, J. Hong, J. E. Kim, S. H. Lee and H. W. Kim, *J. Mater. Chem.,* 2010, **20**, 1907.
32. X. Qi, K. Y. Pu, H. Li, X. Zhou, S. Wu and Q. L. Fan, *Angew. Chem. Int. Ed.,* 2010, **49**, 9426.
33. P. V. Kodgire, A. R. Bhattacharyya, S. Bose, N. Gupta, A. R. Kulkarni and A. Mishra, *Chem. Phy. Lett.,* 2006, **432**, 480.
34. S. B. Jagtap, R. K. Kushwaha and D. Ratna, *J. Appl. Polym. Sci.,* 2013, **127,** 5028.
35. S. B. Jagtap and D. Ratna, *J. Appl. Polym. Sci.,* 2013, **130**, 2610.
36. R. J. Chenn, Y. Zhang, D. Wang and H. Dai, *J. Am. Chem. Soc.,* 2000, **123**, 3838.
37. D. W. Schaefer and R. S. Justice, *Macromolecules,* 2007, **40,** 8501.
38. J. C. Halpin and J. L. Kardos, *Polym. Eng. Sci.*, 1976, **16,** 344.
39. J. J. Liang, Y. Huang, L. Zhang, Y. Wang, Y. F. Ma and T. Y. Guo, *Adv. Funct. Mater.,* 2009, **19,** 2297.
40. X. Zhao, Q. H. Zhang and D. J. Chen, *Macromolecul*es. 2010, **43,** 2357.
41. C. Gomez-Navarro, M. Burghard and K. Kern, *Nano. Lett.,* 2008, **8**, 2045.
42. P. Song, Z. Cao, Y. Cai, L. Zhao, Z. Fang and S. Fu, *Polymer,* 2011, **52**, 4001.
43. G. Galgali, C. Ramesh and A. Lele, *Macromolecules,* 2001, **34**, 852.
44. F. Schedin, A. K. Geim, S. V. Morozov, E. W. Hill, P. Blake and M. I. Katsnelson, *Nat. Mater.,* 2007, **6**, 652.
45. H. W. Chen and F. C. Chang, *Polymer*, 2001, **42**, 9763.
46. D. Ratna, T. Abraham and J. Karger-Kocsis, *Micromole. Chem. Phys.,* 2008, **209**,723.
47. D. Ratna, S. Divekar, A. B. Samui, B.C. Chakraborty and A. K. Banthia, *Polymer*, 2006, **47**, 4068.
48. D. Ratna, T. Abraham, S. Siengchin and J. Karger-Kocsis, *J. Appl. Polym. Sci*.,2008, **110**, 2094.
49. Y. W. Cao, J. C. Feng and P. Y. Wu. *Carbon,* 2010, **48,** 3834.
50. X. Wang, W. Xing, P. Zhang, L. Song, H. Yang and Y. Hua, *Comp. Sci. and Tech.,* 2012, **72,** 737.